Application of S Transform in the Spectral Decomposition of Seismic Data

Mauren Paola Ruthner, Adelson S. de Oliveira, PETROBRAS S/A, Marcelo Gattass, TecGraf PUC-Rio.

Abstract

Spectral Decomposition is a very useful tool for the identification of stratigraphic features, especially in the characterization of thin reservoir. However, Spectral Decomposition is based on the windowed Discrete Fourier Transform, which provides a less optimized time-frequency analysis.
The S Transform differs from the windowed Fourier Transform in the adoption of a window model whose width is adjusted to the frequency that is analyzed. This confers the S Transform properties similar to those of wavelets Transforms in terms of time-frequency resolution.
This paper presents results of the application of the S Transform to the spectral decomposition of synthetic and real seismic data.

Introduction

Hydrocarbon reservoirs tend to extend for hundred of miles but not to be very thick, usually growing thinner at the borders of the reservoir until it disappears. Due to the limitations of the seismic method, thicknesses smaller than the tuning thickness (Widess, 1973) are very difficult to determine.

Partyka et al. (1999) and latter Partyka (2001), proposed a new method for examining thin-bed responses over large 3-D surveys based on Widess' ideas regarding the analysis of the decomposed spectra of seismic data submitted to conventional processing.

The concept behind Partyka's method is that the reflection of a thin bed has a characteristic expression in the frequency domain that is an indication of the temporal bed thickness.

Homogenous thin-bed model

Let us consider the ideal model of a thin and homogenous simple bed with temporal response consisting of two spikes reflectivity of equal but opposite magnitude. The thin bed introduces a predictable periodic sequence of notches into the amplitude spectrum of the composite reflection, as is shown in Figure 1. However, in practice, the seismic wavelet spans multiple subsurface layers, whose reflections interfere with each other resulting in a complex tuned reflection that has a unique expression in the frequency domain.
The amplitude spectrum interference pattern from a tuned reflection is a function of the relationship between the acoustic properties of the sets of layers that comprise the reflectivity function and the thickness of each layer.

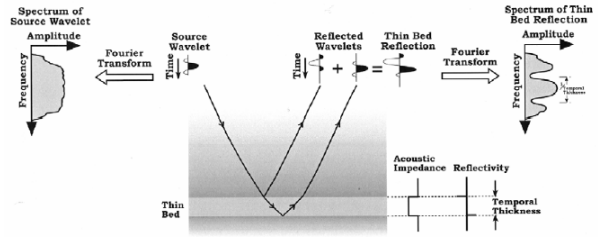

Figure 1 – Thin-bed spectral imaging (from Partyka et al., 1999).

Implications of the analysis window's width

Partyka et al. have verified that there is a significant difference between the amplitude spectra of a long-trace Transform and a short-trace one. For long analysis windows, a succession of geological layers statistically displays a random behavior that, in the context of Partyka et al.'s work, one can approximate to a flat spectrum. Such spectrum, convolved with the source signature's spectrum, results in a spectrum that approximates the spectrum of the source signature (Figure 2).

In short analysis windows, the geology no longer has a random behavior; it ratter acts as a filter. So the resulting spectrum approximates the source signature's overprint plus the local interference pattern representing the acoustic properties and thickness of the geologic layers spanned by the wavelet (Figure 3).

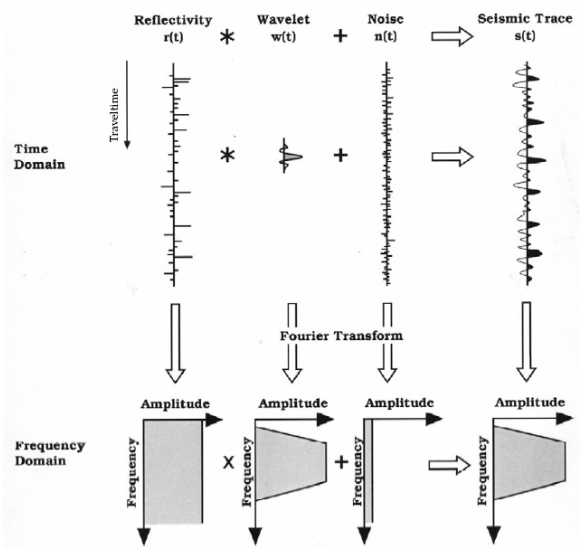

Figure 2 – Long-window spectral decomposition and its relationship with the convolutional model (modified from Partyka et al., 1999).

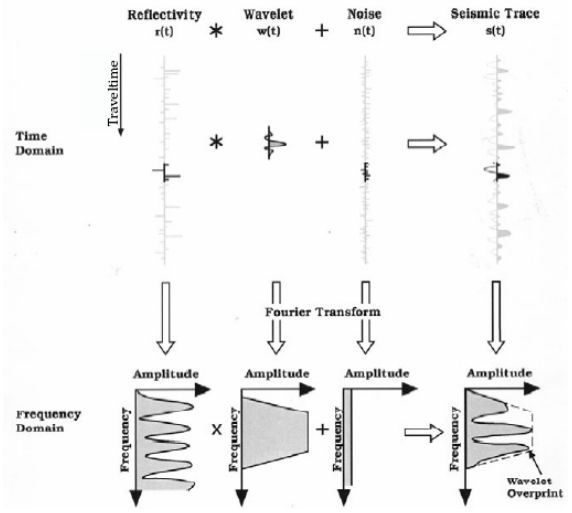

Figure 3 - Short-window spectral decomposition and its relationship with the convolutional model (modified from Partyka et al., 1999).

Partyka et al. have analyzed the short-window spectrum and verified that the pattern of notches occurs at definite periods with respect to frequency. Such periods are determined by the temporal thickness of the layer that was spanned by the wavelet. This relationship is given by the expression below:

$$P_f = \frac{1}{t} \quad (1)$$

where P_f is the period of notches in the amplitude spectrum with respect to frequency (Hz) and t is the temporal thickness of the layer in seconds. In the same way, the value of the frequency component determines the periods of notches in the amplitude spectrum with respect to temporal thickness. So:

$$P_t = \frac{1}{f} \quad (2)$$

where P_t is the period of notches in the amplitude spectrum with respect to the temporal thickness (s) and f is the discrete Fourier frequency (Hz). Besides, the frequency where the first notch occurs is equal to the frequency that corresponds to the period of the notches.

The S Transform

The S Transform (Stockwell et al., 1996) provides a local representation of the amplitude spectrum of a signal. It is defined by the following expression:

$$S(f,\tau) = \int_{-\infty}^{+\infty} h(t) \frac{|f|}{\sqrt{2\pi}} e^{\frac{-(\tau-t)^2 f^2}{2}} e^{-i2\pi ft} dt \quad (3)$$

where $h(t)$ is the signal in the time domain, f is the considered frequency and τ, is the translation. One can see that (3) corresponds to the Fourier Transform except for the multiplicative term

$\left(\frac{|f|}{\sqrt{2\pi}} e^{\frac{-(\tau-t)^2 f^2}{2}} \right)$. This term localizes the events in time and corresponds to a Gaussian window that translates according to τ and scales inversely proportionally to the considered frequency. The scale is given by the standard deviation of the Gaussian function (σ), defined by:

$$\sigma = \frac{1}{|f|} \quad (4)$$

As S Transform corresponds to a representation of the local spectrum of a signal, it can be converted to the Fourier spectrum. This is obtained by integrating the S Transform over $d\tau$:

$$\int_{-\infty}^{\infty} S(\tau,f) d\tau = H(f); f \neq 0 \quad (5)$$

where $H(f)$ is the Fourier Transform of $h(t)$. For $f=0$, the S Transform is defined such that:

$$\int_{-\infty}^{\infty} S(0,\tau) d\tau = H(0); f = 0 \quad (6)$$

Applying the inverse Fourier Transform over (5) and (6) $h(t)$ can be exactly determined from $S(\tau,f)$:

$$h(t) = \int_{-\infty}^{\infty} \left\{ \int_{-\infty}^{\infty} S(f,\tau) d\tau \right\} e^{i2\pi ft} df \quad (7)$$

In Fourier domain, S Transform is obtained by operations over $H(f)$, as follows:

$$S(\tau,f) = \int_{-\infty}^{\infty} H(\alpha+f) e^{\frac{-2\pi^2\alpha^2}{f^2}} e^{i2\pi\alpha\tau} d\alpha; f \neq 0 \quad (8)$$

where α corresponds to translation in the frequency domain.

For discrete data S Transform is computed through a discrete version of (8).

Considering *h[kT]* a discrete time series, where *k = 0, 1, ..., N-1* that corresponds to *h(t)* with a time sampling interval of *T,* the discrete Fourier Transform is given by:

$$H\left[\frac{n}{NT}\right] = \frac{1}{N}\sum_{k=0}^{N-1} h[kT] e^{\frac{-i2\pi nk}{N}} \quad (9)$$

where *n = 0, 1, ..., N-1*.

The set of spanning vectors of the S Transform are not orthogonal and the elements of the S Transform are not independent. Each basis vector of the Fourier Transform is divided by a product into *N* localized vectors, element by element, with the *N* translated Gaussians, such that the sum of the *N* localized vectors is the original basis vector.

Consider equation (8), replacing *f* by $\frac{n}{NT}$, τ by jT and α by $\frac{m}{NT}$ the S Transform of a discrete time series *h [kT]* is then given by:

$$S\left[jT, \frac{n}{NT}\right] = \sum_{m=0}^{N-1} H\left[\frac{m+n}{NT}\right] e^{\frac{-2\pi^2 m^2}{n^2}} e^{\frac{i2\pi mj}{N}}; n \neq 0 \quad (10)$$

For *n=0*, the expression is defined by:

$$S[jT, 0] = \frac{1}{N}\sum_{m=0}^{N-1} h\left(\frac{m}{NT}\right) \quad (11)$$

where *j,m,n=0,1,...,N-1*...

Equation (11) shows that the time series average is in the zero frequency, assuring that the inverse operation will be exact. The expression of the discrete inverse S Transform is given by:

$$h[kT] = \frac{1}{N}\sum_{n=0}^{N-1}\left\{\sum_{j=0}^{N-1} S\left[jT, \frac{n}{NT}\right]\right\} e^{\frac{i2\pi nk}{N}} \quad (12)$$

The same problems of sampling and finite length of the Fourier Transform that are responsible for the implicit periodicity in time and frequency domains, affect the S Transform. In (10) one can see that as $\frac{n}{NT}$ approaches the Nyquist frequency $\left(\frac{1}{2T}\right)$, the term $e^{\frac{-2\pi^2 m^2}{n^2}}$ overlaps into the negative frequencies of $H\left[\frac{m}{NT}\right]$. Stockwell et al.(1996) called this phenomenon *self-aliasing*. According to these authors, *self-aliasing* occurs even when the sampling rate satisfies the Nyquist criteria. At high frequencies the term $e^{\frac{-2\pi^2 m^2}{n^2}}$ become quite wide and *self-aliasing* introduces errors. To avoid this effect, a special Nyquist frequency is proposed. However, when dealing with real time series, as is the case of seismic traces, this effect is avoided by using the analytic signal of the input time series. With this strategy the amplitudes at the negative frequencies to be zeroed, and the *self-aliasing* phenomenon doesn't occur. More details about the special Nyquist frequency can be obtained in Stockwell et al. (1996).

Tests

The models used in the tests presented here simulate reflections of a layer with its top and bottom represented in the time domain by two reflectivity spikes with opposite polarities. The sample rate used was 0.002s (Nyquist frequency = 250Hz) and the record length was 0.720 seconds yielding a frequency increment of 1.190476 Hz. This increment was obtained by inverting the number of points (420) defined for the Fast Fourier Transform - FFT from the library CWP/SU (Cohen et al., 2002).

From equation (2), the 250Hz frequency corresponds to a temporal thickness of 0.004 s. This was the thickness adopted for the first model.

In the first test the model simulates the ideal situation of a layer represented in the time domain by two spikes reflectivity with the same intensity. Figure 4 illustrates the obtained results. Figure 4a shows the input model; in Figure 4b it can be seen the result of the S Transform in terms of time versus amplitude; and Figure 4c presents the results of the S Transform in terms of time versus frequency, with amplitudes represented by a color scale. In Figure 4d the amplitude spectrum for the time sample that corresponds to the middle of the layer is shown. In other words, Figure 4d is a transversal slice of Figure 4c, parallel to the frequency axis. In Figure 4e the amplitude spectrum obtained with the FFT is presented. In Figures, 4b and 4c one can notice that the spectrum was satisfactorily localized in the time domain. The layer has been detected, the energy peak is centered in the middle of the layer and there is a small dispersion at the borders with respect to the initial and final times of the layer. According to equation (2), for a temporal thickness of 0.004s the first notch is expected (excluding the zero frequency) at the 250Hz frequency. Comparing Figures 4d and 4e one can observe that in Figure 4e the first minimum occurred exactly at 250Hz. Regarding the S Transform, in Figure 4d, the spectrum suffered a smoothing.

The second test is similar to the first, except for one modification: the ratio between intensities of the reflectivity spikes that represent the layer's top and bottom was changed from 1/1 to 1/3. The results of this test are shown in Figure 5. Concerning the temporal localization there was a small shift in the energy peak in relation to the middle of the layer, as can be seen in Figures 5b and 5c. In this test, the amplitude spectrum obtained with the S Transform (Figure 5d) has also been smoothed, when compared to the Fourier spectrum (Figure 5e).

In the third test the model tries to simulate a situation closer to real seismic acquisition. The spikes reflectivity were multiplied by a bandpass filter of: 2Hz-5Hz-70Hz-80Hz. The bottom of the layer was not properly sampled and random noise was added to the model, with a signal to noise ratio of 60. The random noise is added to the

signal by multiplying the noise by a factor. This factor (*factor)* is obtained by the following expression:

$$factor = \left(\frac{1}{rs}\right)\left(\frac{amp_{\max}}{\sqrt{amp\sqrt{2}}}\right) \quad (13)$$

where amp_{max} is the maximum amplitude of the trace, *amp* is the amplitude of each sample and *rs* is the signal to noise ratio. In this case a bed thickness obtained with equation (2) was chosen, using as input the maximum frequency (80Hz) before the cutoff. The calculated thickness was 0.0125 s, but it was rounded to 0.014 s to facilitate the analysis. Figure 6 shows the results of this test. Observing Figures 6b and 6c one can notice that, in the time axis, energy was centered in the middle of the layer and, similar to the previous tests, there is a small dispersion at the borders of the layer. In the S Transform spectrum, the smoothing is clearly evident, especially when compared with the Fourier spectrum.

With the purpose of illustrating the technique proposed here, the S Transform was applied to a volume of real data from the Brazilian coast, where the occurrence of channels and fault systems is well known. Figures 7a and 7b show slices of this volume. Arrows indicate channels and faults. Three volumes at constant frequency were generated, with 10Hz, 20Hz and 30 Hz. A time slice was selected from these volumes to be compared with the same time slice obtained form the data volume submitted to conventional processing. Comparing Figure 7c (conventional processing) with 7d (10Hz volume) there seems to exist a continuity in the fault indicated by the yellow arrow. Regarding the channels, in Figure 7e (30Hz volume) it is suggested that the channel indicated by the green arrow is connected. In Figure 7f (20Hz volume) one can observe that inside the selected area more information is visible, suggesting the existence of more channels and faults.

The example with real seismic data shows that although Partyka et al.'s method recovers much more information from data than conventional processing, the analysis of the results must be very rigorous and good knowledge about the geological model involved is required. Therefore, this technique may be more suited to refine an existing model.

Conclusions

The method presented by Partyka et al., 1999 allows the identification of a greater number of seismic events of interest that were not well resolved or even identified in seismic volume submitted to conventional processing. As the complexity of the synthetic models increases, the technique becomes less accurate. Overall, this method seems to be more efficient for qualitative analysis.

The S Transform produces satisfactory results for the localization of events in the time domain. In the spectrum it acts as a smoothing filter. This effect is quite visible in the third test presented here (Figure 6), where the model was contaminated with random noise. In the spectrum the noise was completely smoothed. These effects of the S Transform suggest that the method should be used for qualitative analysis.

References

Widess, M. B., 1973, How thin is a thin bed ? Geophysics, vol. 38, No. 6, pp. 1176-1180.

Partyka, G.; Gridley, J.; Lopez, John., 1999, Interpretational Applications of Spectral Decomposition: The Leading Edge, vol. 18, No. 3, pp. 353-360.

Partyka, G., 2001, Seismic thickness estimation: three approaches, pros and cons.: 71 st. Ann. Internat. Mtg: Soc. of Expl. Geophys. pp. 503-506.

Stockwell, R. G.; Mansinha, L.; Lowe, R. P., 1996, Localization of the Complex Spectrum: The S Transform. IEE Paper: Trans. Signal Processings, vol. 44, pp. 998-1001.

Cohen, J. K. and Stockwell, Jr. J. W., 2002, CWP/SU: Seismic Unix Release 34: a free package for seismic research and processing, Center for Wave Phenomena, Colorado School of Mines.

Acknowledgments

Thanks to Eduardo Lopes de Faria and to Marcos de Carvalho Machado from PETROBRAS, and to Pedro Mário Silva from TecGraf /PUC-RJ for technical support and incentive.

Thanks to colleagues Ana Zélia N. de Barros e Inês S. Vieira for helping in data investigation.

Thanks to the colleague Carlos Eduardo B. S. Abreu for presenting the existent technology and for showing its use in practice.

Thanks to colleagues and manager from Tecnologia Geofísica for technical and operational support.

Thanks to Carolina Alfaro from TecGraf /PUC-RJ for the text's copydesk.

Thanks to PETROBRAS for the permission to publish this work.

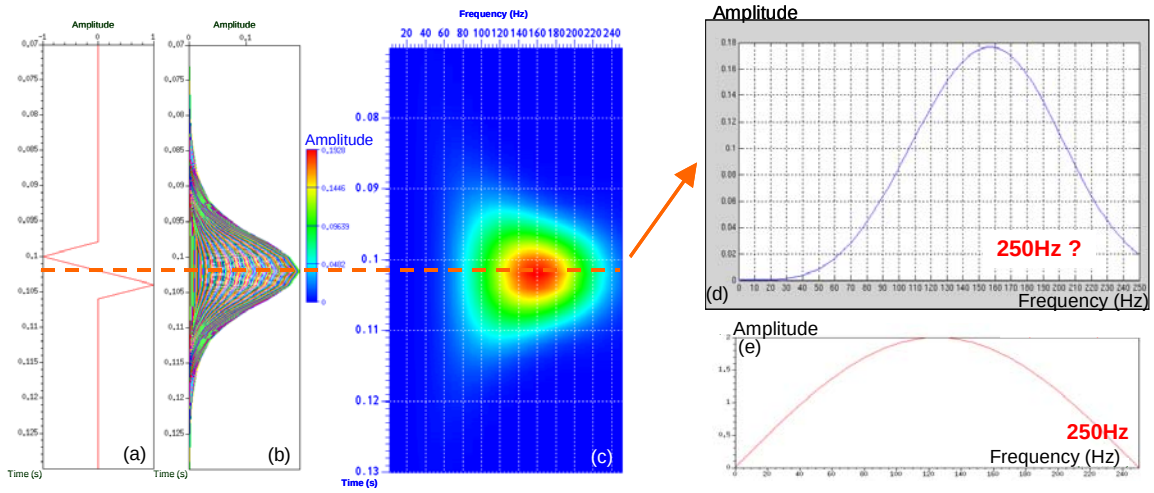

Figure 4 – (a) Layer signature. (b) S Transform: Amplitude x Time. (c) S Transform: Time (s) x Frequencies. (d) S Transform Spectra. (e) Fourier Spectra.

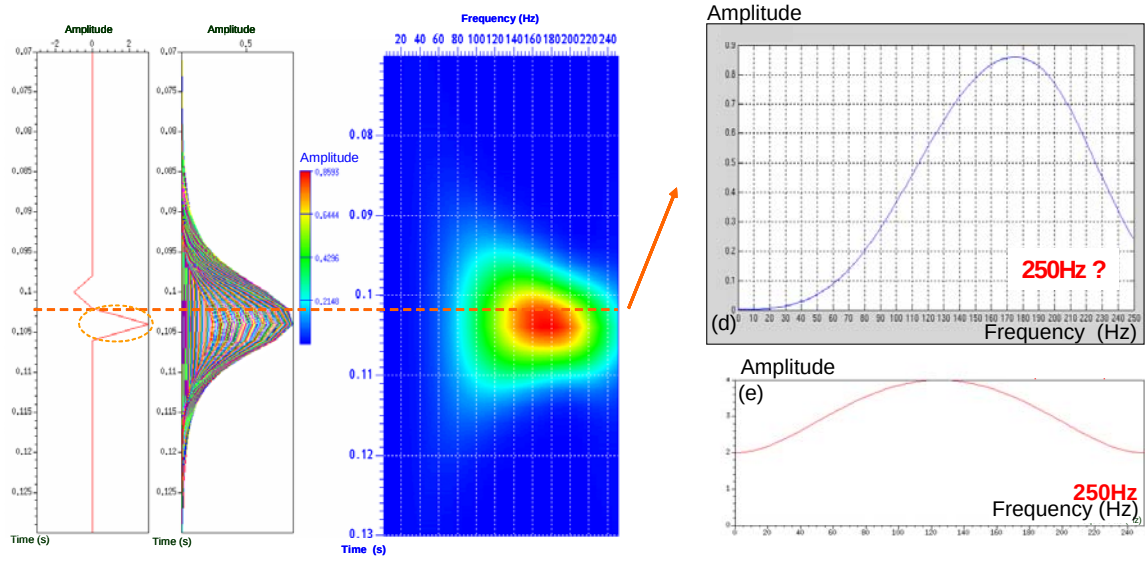

Figure 5 – (a) Layer signature. (b) S Transform: Amplitude x Time. (c) S Transform: Time (s) x Frequencies. (d) S Transform Spectra. (e) Fourier Spectra.

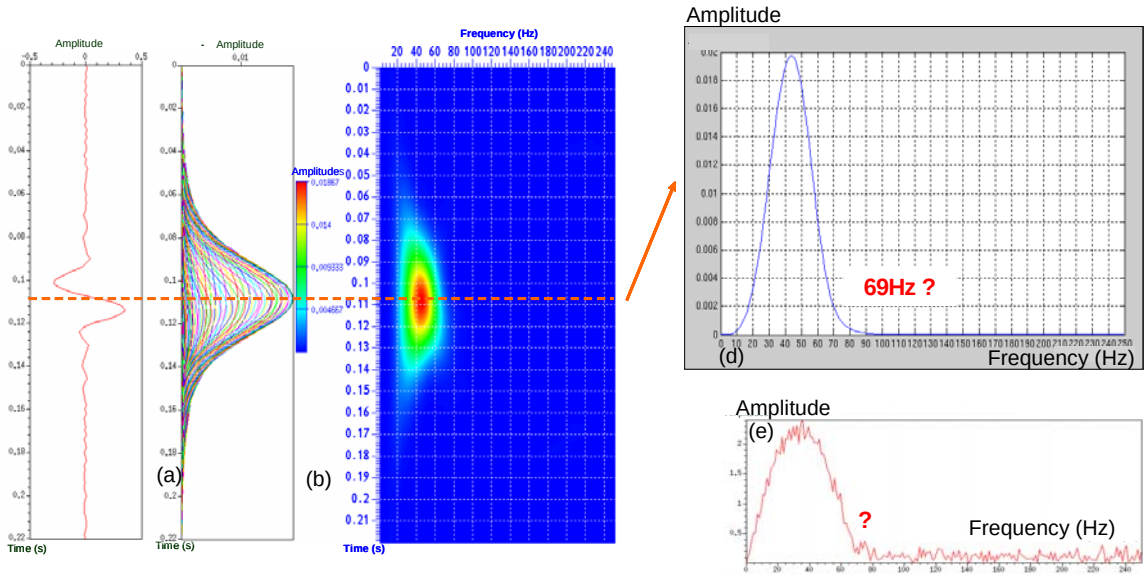

Figure 6 – (a) Layer signature. (b) S Transform: Amplitude x Time. (c) S Transform: Time (s) x Frequencies. (d) S Transform Spectra. (e) Fourier Spectra.

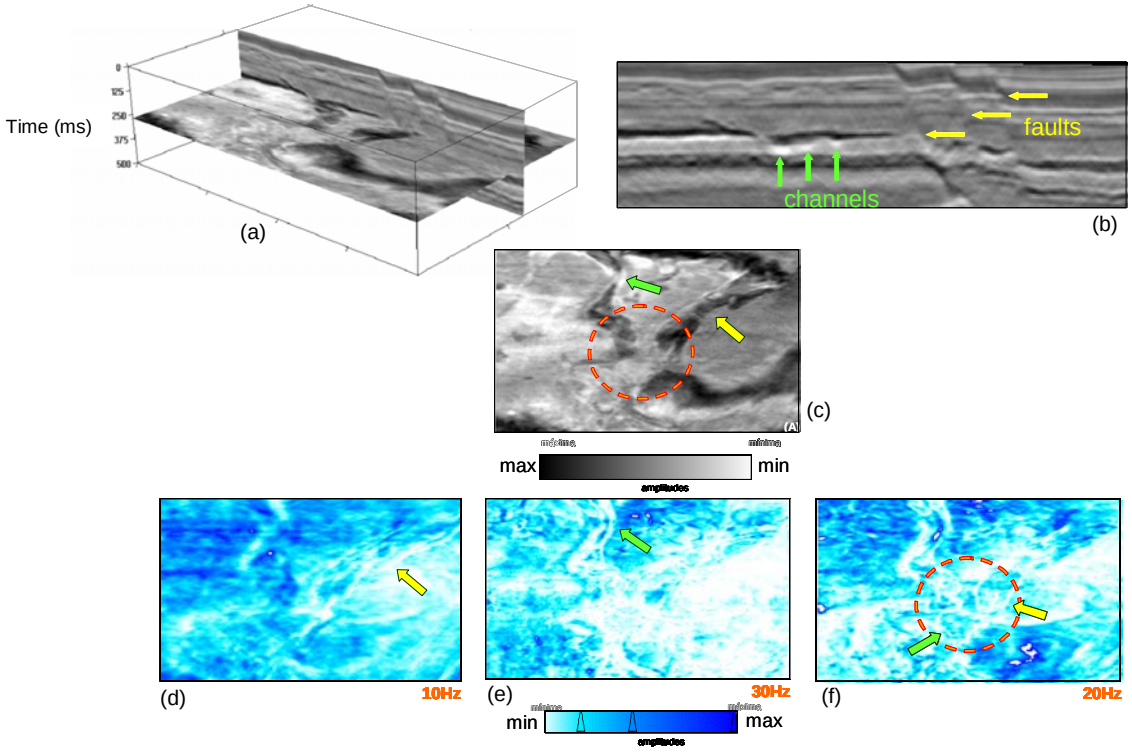

Figure 7 – (a) Location of the slices in the original volume. (b) Channels and faults in the cross section. (c) Time slice. (d) 10Hz volume. (e) 30Hz volume. (f) 20Hz volume.